IEEE Photonics Journal
An IEEE Photonics Society Publication

Open Access

Study on the k-Connectivity of UV Communication Network Under the Node Distribution of RWP Mobility Model in the Arbitrary Polygon Area

Volume 12, Number 4, August 2020

Cheng Li
Jianhua Li
Zhiyong Xu
Jingyuan Wang

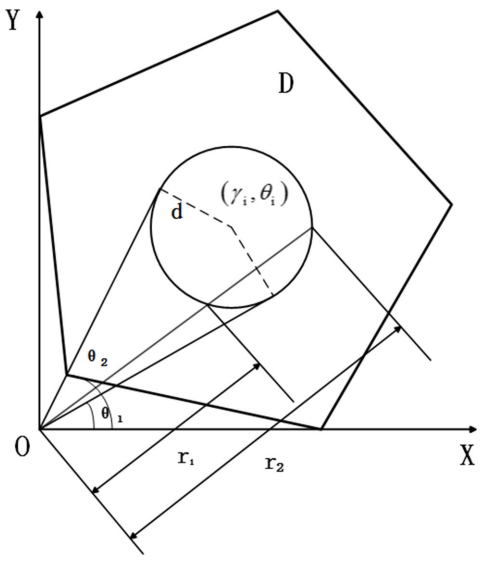

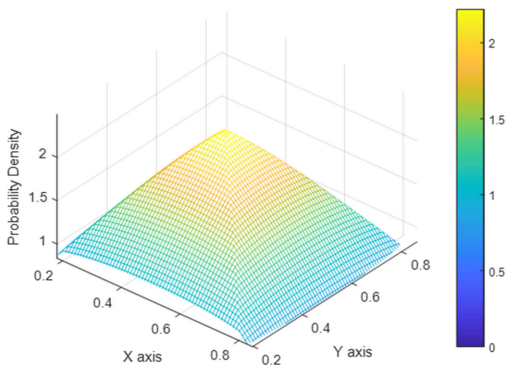

DOI: 10.1109/JPHOT.2020.3003896

Study on the k-Connectivity of UV Communication Network Under the Node Distribution of RWP Mobility Model in the Arbitrary Polygon Area

Cheng Li, Jianhua Li, Zhiyong Xu, and Jingyuan Wang

College of Communication Engineering, Army Engineering University of PLA, Nanjing, China

DOI:10.1109/JPHOT.2020.3003896

Manuscript received May 26, 2020; revised June 12, 2020; accepted June 17, 2020. Date of current version July 14, 2020. This work was supported by the National Natural Science Foundation of China (61975238), and in part by the Research Center of Optical Communications Engineering & Technology, Jiangsu Province (ZXF201901). Corresponding authors: Jianhua Li (e-mail: ljhice@163.com), Zhiyong Xu (e-mail: njxzy123@163.com), Jingyuan Wang (e-mail: wjywjy2011@163.com).

Abstract: This manuscript studies on the k-connectivity (k = 1, 2, 3) of ultraviolet (UV) non-line-of-sight (NLOS) communication network in the arbitrary polygon area where the nodes move according to random waypoint (RWP) mobility. In the paper, based on the relationship between the path loss and the transceiver elevation angles, the change of the communication radii of the UV nodes can be analyzed. Besides, a series of parameters that affect the UV network connectivity probability are numerically researched like node density, transmission power and data rate. The results illustrate that performance of communication mode with small elevation angle is better than that of mode with large elevation angle in the arbitrary polygon area. Furthermore, the 2-connectivity with better robustness in a square area is numerically compared with that in a circular area, and then the network parameters that meet the actual applications are clearly given.

Index Terms: Arbitrary polygon area, K-connectivity, random waypoint (RWP), wireless ultraviolet (UV) network.

1. Introduction

At present, the technology fusion of ultraviolet (UV) communication and Ad Hoc network, making it an ideal means to meet the communication needs of complex electromagnetic environments such as disaster sites, has become a new research hotspot at home and abroad. On the one hand, the UV light source has the advantages of high confidentiality, non-line-of-sight (NLOS) communication and strong anti-interference [1]. These characteristics are rarely available in other signal sources. On the other hand, it can overcome the shortcomings of huge UV communication loss and short communication distance by using Ad Hoc network.

For many years, domestic and foreign scholars have been devoted to the research of UV communication, hoping to make a breakthrough in practical applications. Vavoulas *et al.* [2] pointed out that node density (ρ), transmission power (P_t) and data rate (R_b) are the main parameters that affect the performance of UV communication. In Ref. [3], the relationship between the various transceiver angles and the path loss parameters was accurately measured through multiple experiments. Ref. [4] analyzed the impact of the transceiver elevation angle on the communication

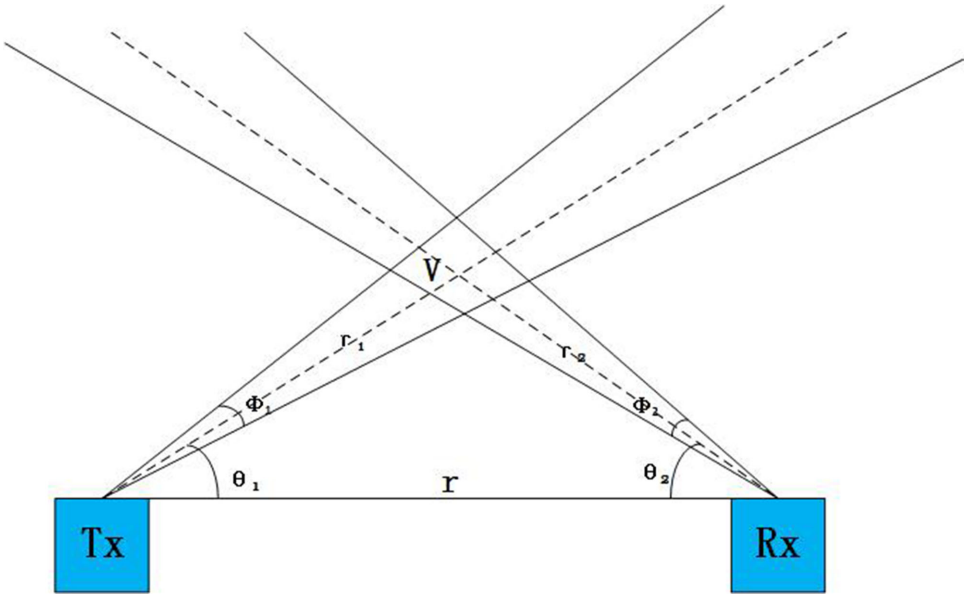

Fig. 1. UV NLOS communication model.

performance in the 1-connected network state, but it did not analyze the network performance under multiple connectivity state. And the model of this literature is a static model with uniformly distributed nodes. In practical applications, UV nodes are mostly arranged in mobile terminals. Ref. [5] discussed the influences of the performance parameters on network connectivity under multiple connectivity networks, but only analyzed the NLOS(a) (vertical transmission and vertical reception) communication mode of UV. Moreover, the network models discussed above are all built under specific shape conditions and are only applicable to circular areas.

In this manuscript, the network model is established in an irregular shape where the nodes move according to random waypoint (RWP) mobility. Under the arbitrary polygon region and different elevation angles of receiving and transmitting ends, the influences of the communication parameters on the connectivity performance under multiple connectivity state are analyzed. In addition, the model is compared with the uniform distribution model of circular area and polygon area, and the differences among the three are analyzed.

The rest of the paper is structured as follows. Section II presents a brief description of the UV communication model and the influences of elevation angles on the communication radius. In Section III, the approximate probabilities of k-connectivity are derived in the arbitrary polygon area according to the RWP motion model. The simulation results are analyzed and compared in Section IV. At the end, we summarize and reach the relevant conclusions in Section V.

2. Preliminaries

2.1 UV Communication Model

Fig. 1 shows the UV NLOS communication model [7]. In this figure, Φ_1 is the beam divergence angle, θ_1 is the transmission elevation angle, Φ_2 is the field-of-view (FOV) angle, θ_2 is the reception elevation angle, *V* is the effective scatterer, and *r* is the communication distance [8].

2.2 UV Communication Radius

At short distances below a few kilometers, Chen *et al.* [9] took a lot of experimental data as a reference and proposed a UV communication path loss model. Through their physics experiment platform, their team recorded large amounts of experimental data on path loss under different

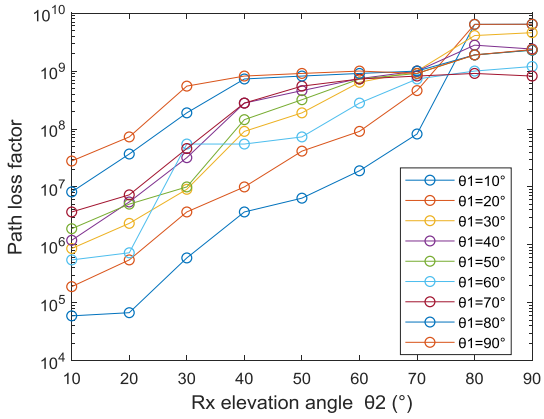

Fig. 2. Transceiver elevation angles and path loss factor.

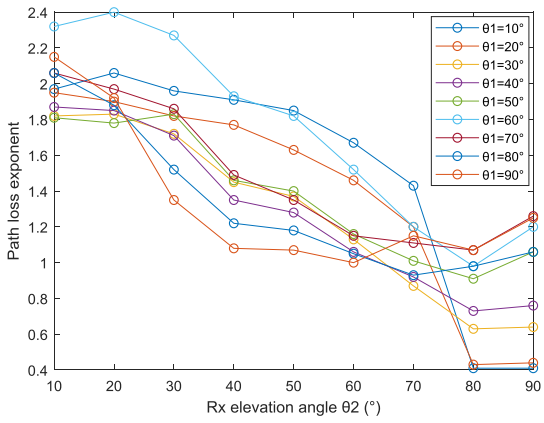

Fig. 3. Transceiver elevation angles and path loss exponent.

transceiver elevation angles when Φ_1 and Φ_2 are fixed at 17° and 30°. According to the theory proposed by Chen, the path loss model is

$$L = \xi r^{\alpha}, \tag{1}$$

where α is the loss exponent, ξ is the loss factor, r is the distance. Based on Chen's experiment, the relationship between elevation angles and loss parameters was found through a lot of simulation. It has been shown in Fig. 2 and Fig. 3.

When using Poisson noise model, the UV communication radius for on-off keying is derived as [10], [11]

$$R_{OOK} = \sqrt[\alpha]{-\frac{\eta\lambda P_t}{hc\xi R_b \ln(2P_e)}}, \tag{2}$$

where λ is the wavelength, η is the quantum efficiency of the filter and photodetector, P_t is the transmission power, R_b is the data rate, P_e is the bit error rate, c is the speed of light, $c = 3.0 * 10^8$m/s, h is the Planck constant, $h = 6.62 * 10^{-34}$J•s. In Eq. (2), we got the relationship between communication parameters and the communication radius.

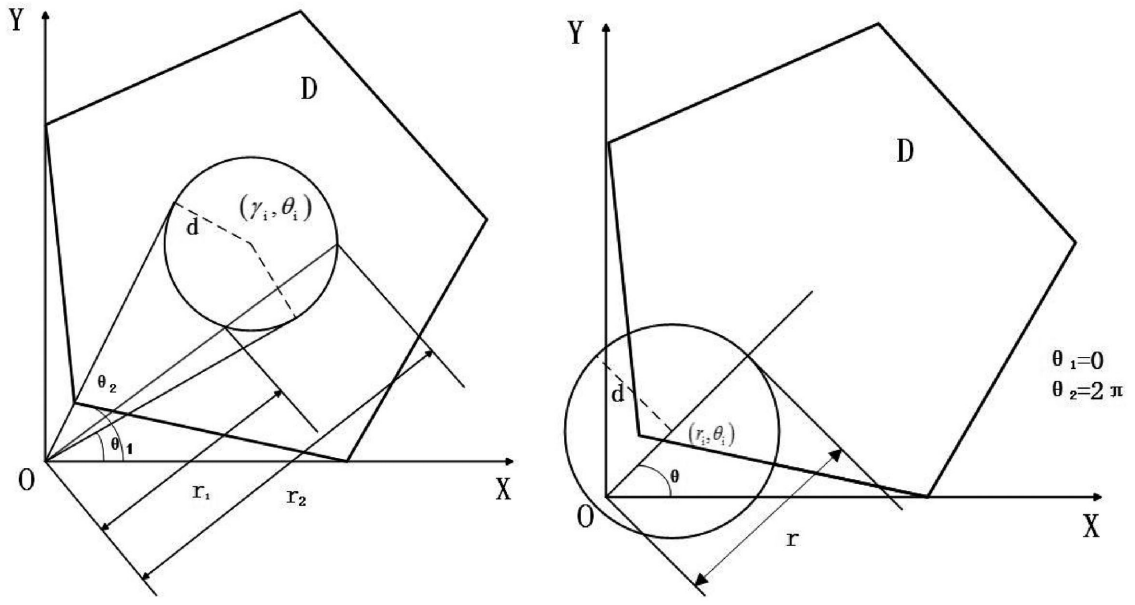

(a) : $r \geq d$ (b) : $r < d$

Fig. 4. Polygonal network model.

3. K-Connectivity

In this article, the UV network connectivity starts with a two-dimensional network. The UV k-connected network means that k mutually independent paths exist in the network. Even if $k-1$ links are broken in the network, there are still available links between any nodes [8].

The motion of the UV nodes is according to the RWP model, and the RWP model is the most commonly used model for describing node motion in Ad hoc networks, which describes the movement of nodes within a given region [12]. This model decomposes the entire node movement process into a series of pause and move alternating processes. The node stays at a position for a certain time and then moves to the next randomly selected destination. Due to the influence of boundary effects, when the RWP motion model reaches a steady state, the nodes in the network will show a non-uniform distribution.

When the distribution of network nodes reaches steady state according to the RWP model in an arbitrary polygon area D, and the area of the polygon is A, the probability density function (PDF) of the node located in the region is

$$f_{XY}^{D}(x, y) = \begin{cases} f_{XY}(x, y) & (x, y) \in D \\ 0 & \text{else} \end{cases}. \tag{3}$$

For the arbitrary node $i(r_i, \theta_i)$ in the network, its communication coverage area $B_d(r_i, \theta_i)$ is a circle with (r_i, θ_i) as the center and d as the radius. Its equation can be expressed as

$$(r\cos\theta - r_i\cos\theta_i)^2 + (r\sin\theta - r_i\sin\theta_i)^2 = d^2. \tag{4}$$

Simplify equation 4, we can get a quadratic equation in one unknown with r

$$r^2 - 2r\left(r_i\cos\theta_i\cos\theta + r_i\sin\theta_i\sin\theta\right) + \left(r_i^2 - d^2\right) = 0. \tag{5}$$

If the distance between the node i and origin O is same to or longer than the radius d, that is $r \geqslant d$ as Fig. 4(a),

Solving Eq. (5), we can derive that

$$\begin{cases} \theta_1 = \arcsin\left(\frac{r_i \sin\theta_i}{r_i}\right) - \arcsin\left(\frac{d}{r_i}\right) \\ \theta_2 = \arcsin\left(\frac{r_i \sin\theta_i}{r_i}\right) + \arcsin\left(\frac{d}{r_i}\right) \\ r_1 = r_i\cos\theta_i\cos\theta + r_i\sin\theta_i\sin\theta \\ -\sqrt{(r_i\cos\theta_i\cos\theta + r_i\sin\theta_i\sin\theta)^2 - (r_i^2 - d^2)} \\ r_2 = r_i\cos\theta_i\cos\theta + r_i\sin\theta_i\sin\theta \\ +\sqrt{(r_i\cos\theta_i\cos\theta + r_i\sin\theta_i\sin\theta)^2 - (r_i^2 - d^2)} \end{cases}. \tag{6}$$

θ_1 and θ_2 , r_1 and r_2 represent the upper and lower bounds of the integral area in the polar coordinate system, respectively. When $r < d$, as Fig. 4(b), the origin O is in the range of the area $B_d(r_i, \theta_i)$,

$$\begin{cases} \theta_1 = 0 \\ \theta_2 = 2\pi \\ r_1 = 0 \\ r_2 = r_i\cos\theta_i\cos\theta + r_i\sin\theta_i\sin\theta \\ +\sqrt{(r_i\cos\theta_i\cos\theta + r_i\sin\theta_i\sin\theta)^2 - (r_i^2 - d^2)} \end{cases}. \tag{7}$$

For the area D, we need to calculate the probability $p(r_i, \theta_i, \mathrm{d})$ of any other nodes falling into $B_d(r_i, \theta_i)$,

$$p(r_i, \theta_i, d) = \begin{cases} \int_{r_1}^{r_2} dr \int_{\theta_1}^{\theta_2} f_{XY}^D(r\cos\theta, r\sin\theta) r d\theta, & r_i \geq d \\ \int_{r_1}^{r_2} dr \int_{\theta_1}^{\theta_2} f_{XY}^D(r\cos\theta, r\sin\theta) r d\theta & r_i < d \end{cases}. \tag{8}$$

Since all UV network nodes are independent of each other, other nodes within the area $B_d(r_i, \theta_i)$ obey a binomial distribution $Bin(n-1, p(r_i, \theta_i, d))$. In the area D, the probability that any other node is outside $B_d(r_i, \theta_i)$ is $1 - p(r_i, \theta_i, \mathrm{d})$, and the probability of a given node having k adjacent nodes is [5]

$$P_k(r_i, \theta_i, d) = \binom{n-1}{k} \cdot p(r_i, \theta_i, d)^k \cdot (1 - p(r_i, \theta_i, d))^{n-1-k}. \tag{9}$$

Hence, what has at least k adjacent nodes is [5]

$$P_{\geq k}(r_i, \theta_i, d) = 1 - \sum_{i=0}^{k-1} \binom{n-1}{i} \cdot p(r_i, \theta_i, d)^i \cdot (1 - p(r_i, \theta_i, d))^{n-1-i}. \tag{10}$$

So, we derived the probability that any node in the arbitrary polygon area D has at least k adjacent nodes [5]

$$Q_{n,\geqslant k}(d) = \iint_D f_{XY}^D(r\cos\theta, r\sin\theta) P_{\geqslant k}(r_i, \theta_i, d) r \mathrm{d}\theta \mathrm{d}r. \tag{11}$$

In the UV networks, the node degree d is the number of neighbor nodes connected to the node. In practical applications, we usually use the probability that each node has at least k adjacent nodes to approximate the k connected probability [13],

$$P(G \text{ is } k\text{−connected}) \approx P(d_{\min} \geq k). \tag{12}$$

Therefore, we derived the UV k-connectivity probability as

$$P(G \text{ is } k\text{−connected}) \approx P(d_{\min} > k) = (Q_{n,\geq k}(d))^n \tag{13}$$

By substituting (2), (3), (8), (10), (11) into (13), we can calculate the connectivity probability of UV network through a series of communication parameters.

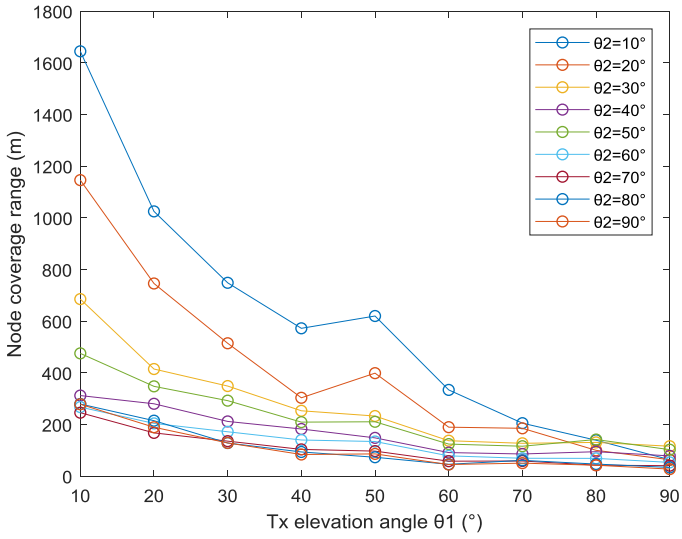

Fig. 5. Relationship between communication radii and transceiver elevation angles.

4. Simulation and Analysis

At the beginning of this section, the change trend of the communication radii with transceiver elevation angles is accurately simulated. Then, the influences of main communication parameters on network connectivity were analyzed under the condition of different transmitting and receiving end elevation angles. Finally, the differences between nodes in an arbitrary polygon according to the RWP motion model and uniform distribution in any shape are compared. In the simulation process, we choose $\Phi_1 = 17°$, $\Phi_2 = 30°$, $\lambda = 250$ nm, $\eta = 0.045$, $P_e = 10^{-6}$.

4.1 Elevation Angles and Communication Radii

Through the simulation of Eq. (2), we can analyze the effect of elevation angles on the node coverage range. The change trend of the communication radii with transceiver elevation angles is shown as in Fig. 5. ($R_b = 10$ kbps, $P_t = 0.5$ w)

It is found from Fig. 5 that the trend of the communication radius changing with the elevation angle is approximately the same. When the transmission elevation angle or the reception elevation angle becomes larger, the communication radius decreases.

By comparison, it can be seen that when the transmitting end elevation angle is 50°, the node coverage range is greater than the range when elevation angle is 40°. Since the volume of the effective scatterer V becomes larger as θ_1 increases ($\Phi_1 = 17°$, $\Phi_2 = 30°$), and the node coverage range increases. When θ_1 exceeds 50°, the range gain caused by the increase of the effective scatterer V is not enough to offset the path loss caused by larger θ_1. And this provides a reference for the selection of angles in the next simulation.

4.2 The Connectivity Properties

The square area was selected for experimental simulation in this manuscript, and the square side length was 1000 m. In the simulation, 100000 topological graphs were generated according to different network parameters, and the number of network topologies with k-connected (k = 1, 2, 3) characteristics is calculated respectively, and then the ratio of the numerical value to the total (100000) is approximated as the probability of network connectivity.

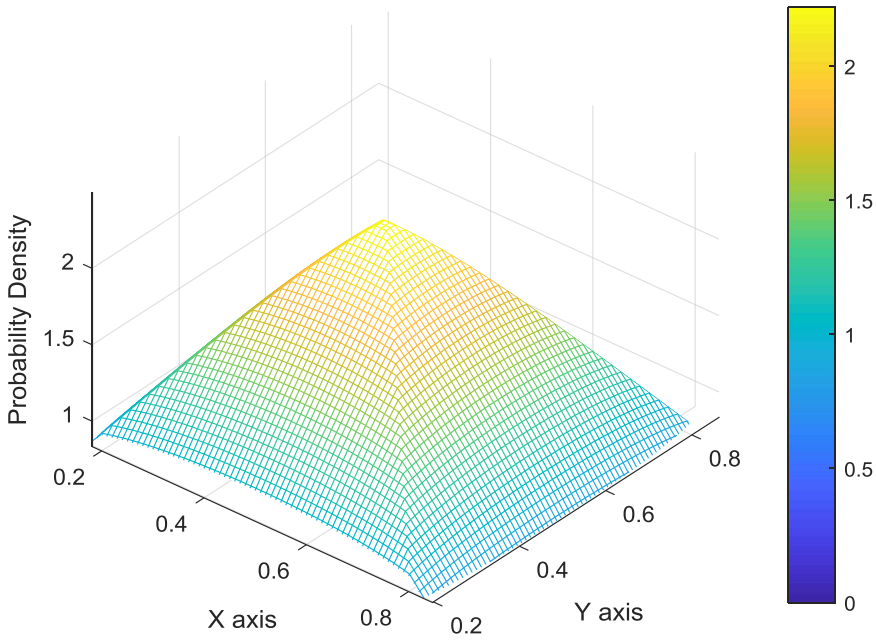

Fig. 6. Node distribution obtained by simulation.

In a square region, the nodes obey the RWP motion model, and then the pdf of the nodes is related to the pause time t_p and the speed v of the nodes. The pdf is [14], [15]

$$f_{RWP}^{D}(x,y)=\begin{cases} P_{\text{pause}}+\left(1-P_{\text{pause}}\right)f(x,y) & \text{if } (x,y)\in[0,1000]^2 \\ 0 & \text{else} \end{cases}. \tag{14}$$

In Eq. (14),

$$P_{\text{pause}}=\frac{t_p}{t_p+\frac{0.521405}{v}}. \tag{15}$$

$$f(x,y)=6y+\frac{3}{4}\left(1-2x+2x^2\right)\left(\frac{y}{y-1}+\frac{y^2}{(x-1)x}\right) +\frac{3y}{2}\left[(2x-1)(y+1)\ln\left(\frac{1-x}{x}\right)+\left(1-2x+2x^2+y\right)\ln\left(\frac{1-y}{y}\right)\right] \tag{16}$$

Where the value range of (x, y) is

$$D^{*}=\left\{(x,y)\in[0,1]^2\,|\,(0<x\leqslant 500)\wedge(0<y\leqslant x)\right\}, \tag{17}$$

The pdf of $f(x, y)$ in the rest of the square area can be obtained by symmetry,

$$f(x,y)=f(\mathrm{y},\mathrm{x})=f(1-\mathrm{x},\mathrm{y})=f(\mathrm{x},1-\mathrm{y}). \tag{18}$$

In the simulation of this article, the selected pause time t_p is 0, we derived

$$f_{RWP}^{D}(x,y)=\begin{cases} f(x,y) & \text{if } (x,y)\in[0,1000]^2 \\ 0 & \text{else} \end{cases}. \tag{19}$$

Through simulation, we got the 3D plot of the node distribution.

In the analysis of 4.1, we knew that when the reception elevation angle is large, the node communication radius varies little with angle, and when the reception elevation angle is small, the radius varies widely. Thus, when comparing the impact of main communication parameters on

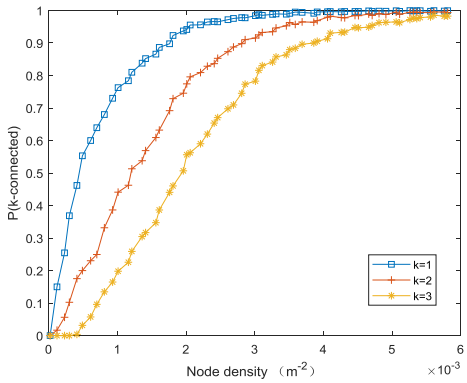

(a) NLOS-a θ_1=90°, θ_2=90°

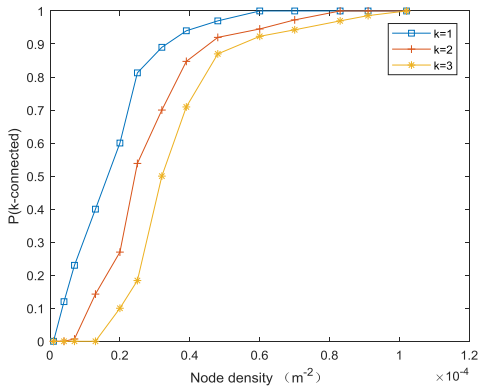

(b) NLOS-b θ_1=30°, θ_2=90°

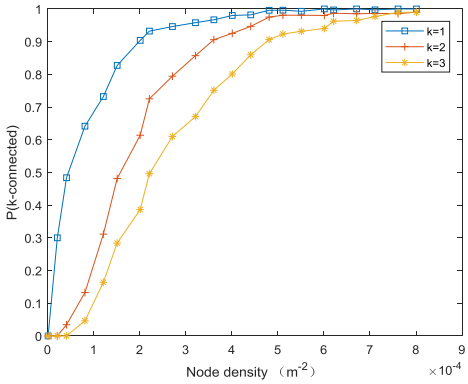

(c) NLOS-b θ_1=50°, θ_2=90°

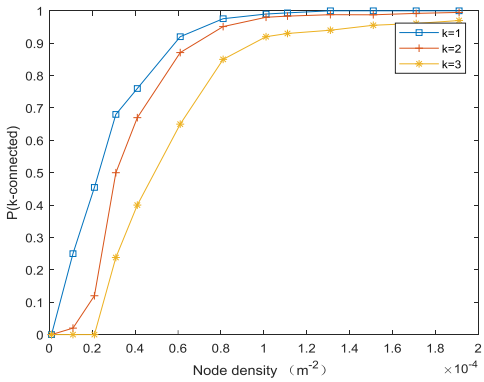

(d) NLOS-c θ_1=30°, θ_2=50°

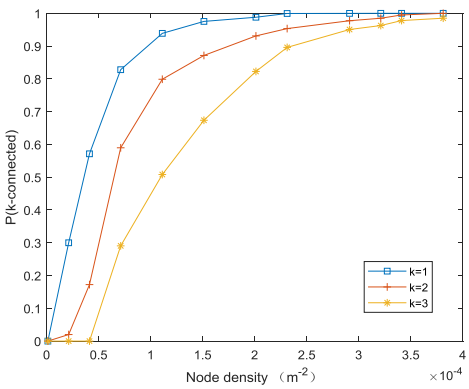

(e) NLOS-c θ_1=50°, θ_2=50°

Fig. 7. Relationship between network connectivity and node density: (a) NLOS-a $\theta_1 = 90°$, $\theta_2 = 90°$, (b) NLOS-b $\theta_1 = 30°$, $\theta_2 = 90°$, (c) NLOS-b $\theta_1 = 50°$, $\theta_2 = 90°$, (d) NLOS-c $\theta_1 = 30°$, $\theta_2 = 50°$, (e) NLOS-c $\theta_1 = 50°$, $\theta_2 = 50°$.

the network connectivity probability, the selected combinations of transceiver elevation angles are NLOS(a) (vertical transmission and vertical reception, $\theta_1 = 90°$, $\theta_2 = 90°$), NLOS(b) (non-vertical transmission and vertical reception, $\theta_1 = 30°$, $\theta_2 = 90°$; $\theta_1 = 50°$, $\theta_2 = 90°$) and NLOS(c) (non-vertical transmission and non-vertical reception, $\theta_1 = 30°$, $\theta_2 = 50°$; $\theta_1 = 50°$, $\theta_2 = 50°$).

First of all, Fig. 7 illustrates that the effect of the node density on network connectivity for different transceiver elevation angles under the same $P_t = 0.5$ W, $R_b = 10$ kbps. The nodes moved according to RWP motion model in a square region. A similar performance is shown on different transceiver elevation angles. We observe that the k-connected probability increases as the

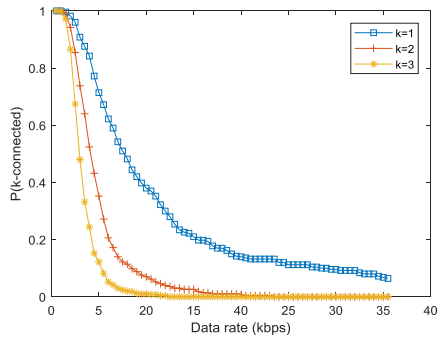

(a) NLOS-a θ_1=90°, θ_2=90°

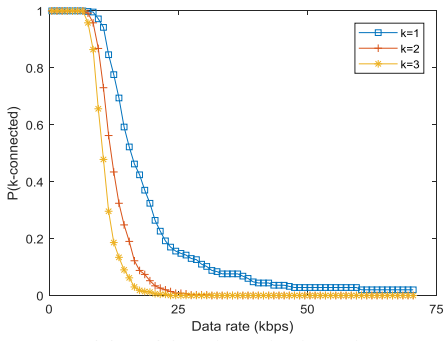

(b) NLOS-b θ_1=30°, θ_2=90°

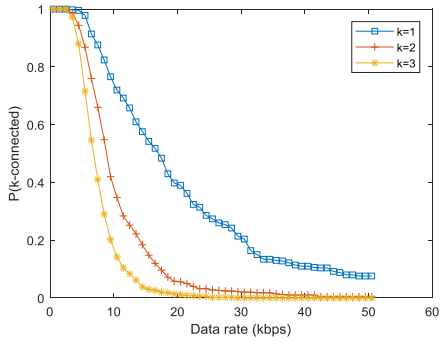

(c) NLOS-b θ_1=50°, θ_2=90°

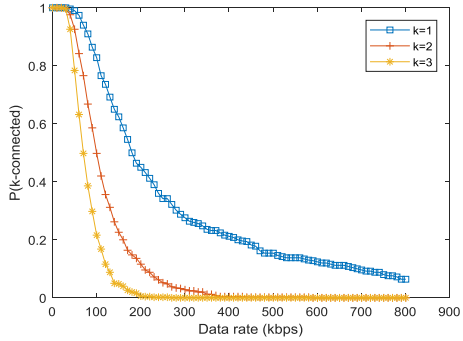

(d) NLOS-c θ_1=30°, θ_2=50°

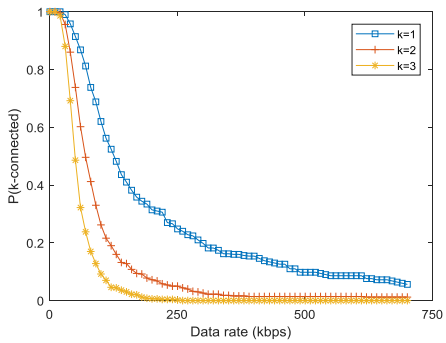

(e) NLOS-c θ_1=50°, θ_2=50°

Fig. 8. Relationship between network connectivity and data rate: (a) NLOS-a $\theta_1 = 90°$, $\theta_2 = 90°$, (b) NLOS-b $\theta_1 = 30°$, $\theta_2 = 90°$, (c) NLOS-b $\theta_1 = 50°$, $\theta_2 = 90°$, (d) NLOS-c $\theta_1 = 30°$, $\theta_2 = 50°$, (e) NLOS-c $\theta_1 = 50°$, $\theta_2 = 50°$.

node density increases. Hence, more UV nodes are required in order to obtain better connectivity. By comparing the results in Fig. 7, the communication radius is the smallest in the NLOS(a) communication mode. When 2-connected network probability achieves 95%, ρ is $3.41{*}10^{-3}$ m^{-2}, and 3410 nodes are needed in a plane square with a side length of 1000m. When transmitting elevation angle 50°, the node density of the same connectivity probability is $4.51{*}10^{-4}$ m^{-2}, which is only 13.2% of NLOS(a). Comparing Fig. 7(a), (b), (c), (d) and (e), it can be seen that more nodes need to be deployed for the 3-connected network than that of 2-connected network. A higher node density, about 37.5%, is needed to reach 3-connectivity as compared with 2-connectivity, for a given connectivity probability in NLOS(a). And the proportion increases to 40.5% from 1-connectivity to 2-connectivity. It provides theoretical guidance for the parameter setting in the subsequent UV networking.

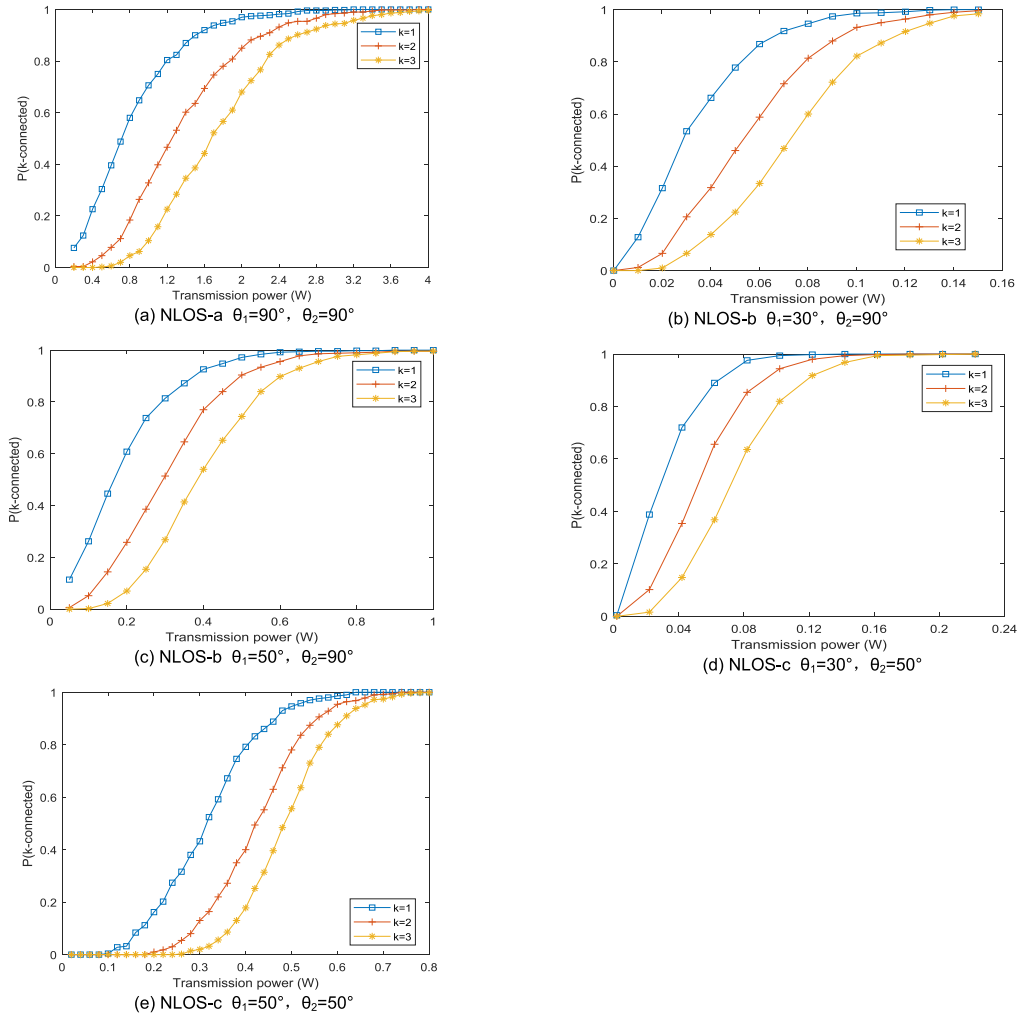

Fig. 9. Relationship between network connectivity and transmission power: (a) NLOS-a $\theta_1 = 90°$, $\theta_2 = 90°$, (b) NLOS-b $\theta_1 = 30°$, $\theta_2 = 90°$, (c) NLOS-b $\theta_1 = 50°$, $\theta_2 = 90°$, (d) NLOS-c $\theta_1 = 30°$, $\theta_2 = 50°$, (e) NLOS-c $\theta_1 = 50°$, $\theta_2 = 50°$.

Figs. 8 and 9 illustrate the multi-connected probability against P_t and R_b, respectively. The node density selected in this section is $5.0{*}10^{-4}$ m^{-2}. When P_t increases or R_b decreases, the communication range increases. And then the UV network k-connectivity also increases. Comparing Fig. 8 and Fig. 9, we observe the network status of NLOS(c) surpasses that of NLOS(a) and NLOS(b) under the same P_t and supported R_b. In NLOS(c), Fig. 8(d) indicates the R_b reduction from 1-connectivity to 2-connectivity is approximately 32.5%, whereas this percentage is dropped to 22.0% from 2-connectivity to 3-connectivity ($\theta_1 = 30°$, $\theta_2 = 50°$). Fig. 9(d) shows that about 34.1% more P_t needs to be increased to get from 1-connectivity to 2-connectivity, whereas this percentage is dropped to 18.5% from 2-connectivity to 3-connectivity ($\theta_1 = 30°$, $\theta_2 = 50°$).

4.3 2-Connectivity Analysis for Three Distribution Regions

Multiple connectivity is usually required among UV nodes in order to obtain higher reliability. The 2-connected network has better robustness and does not require excessive energy consumption. In our previous research, in order to simplify the model and reduce the difficulty of simulation, we

TABLE 1
2-Connectivity Analysis for Three Distribution Regions

Node distribution	Evenly distributed in a circular area			Evenly distributed in a square area			RWP Mobility Model in a square area		
UV parameters	Node density (m^{-2}) Rb=10 kbps P_t=0.5W	Transmission power (W) ρ=5.0*10^{-4} m^{-2} Rb=10 kbps	Data rate (kbps) ρ=5.0*10^{-4} m^{-2} Pt=0.5W	Node density (m^{-2}) Rb=10 kbps Pt=0.5W	Transmission power (W) ρ=5.0*10^{-4} m^{-2} Rb=10 kbps	Data rate (kbps) ρ=5.0*10^{-4} m^{-2} Pt=0.5W	Node density (m^{-2}) Rb=10 kbps Pt=0.5W	Transmission power (W) ρ=5.0*10^{-4} m^{-2} Rb=10 kbps	Data rate (kbps) ρ=5.0*10^{-4} m^{-2} Pt=0.5W
NLOS(a) θ 1=90° θ 2=90°	4.51*10^{-3}	2.24	3.11	1.71*10^{-3}	1.12	4.41	3.41*10^{-3}	2.51	2.49
NLOS(b) θ 1=30° θ 2=90°	1.95*10^{-4}	0.32	18.51	1.78*10^{-4}	0.26	21.82	2.51*10^{-4}	0.59	10.81
NLOS(b) θ 1=50° θ 2=90°	4.32*10^{-4}	0.52	12.83	2.20*10^{-4}	0.31	18.11	4.51*10^{-4}	0.61	7.88
NLOS(c) θ 1=30° θ 2=50°	3.51*10^{-5}	0.09	43.10	2.95*10^{-5}	0.06	53.01	6.20*10^{-5}	0.13	34.5
NLOS(c) θ 1=50° θ 2=50°	6.50*10^{-5}	0.31	18.71	4.32*10^{-5}	0.28	33.20	8.32*10^{-5}	0.22	20.7

selected a model with uniformly distributed UV nodes in the circular area for research (Ref. [8]). With the deepening of our learning, in order to get closer to the reality, we continue to optimize and improve the model, and then there is a model with uniformly distributed UV nodes in arbitrary polygons and a model with UV nodes moving in arbitrary polygons. By comparing the impact of communication parameters on the UV networks, we numerically compared the connectivity of the three distribution methods under the square area and the circular area, and then the appropriate parameter settings for 2-connectivity were shown as Table 1.

Under the same condition that the 2-connectivity probability reaches 95%, Table 1 presents a numerical example for the ρ, P_t and R_b. The numerical results show that mobility reduces the connectivity probability of the network. In the three models, when the UV nodes move in the square area according to the RWP model, ρ and P_t required to meet the network 2-connection are higher than the static circular and square uniform distribution models, and R_b is also less than the other two models. The square uniform distribution model is the easiest to reach the network 2-connectivity. The performance of the circular uniform distribution model is somewhere in between.

Since the "border effect" of the circular area is stronger, there are more nodes in the edge range, and the connected areas of these nodes are smaller [16]. We note that the parameter settings under the uniform distribution of nodes in the circular area are more demanding than that of the square area. In the square area, due to the uneven distribution of nodes under the RWP motion model, the connectivity effect is worse than that of under the uniform distribution condition.

5. Conclusion

In this paper, the influence of the transceiver elevation angle, ρ, P_t and R_b on the UV network connectivity are numerically researched under the RWP motion model of nodes in the arbitrary polygon. We observe the communication radius decreases when the transceiver angle becomes larger. The network status of NLOS(c) surpasses that of NLOS(a) and NLOS(b) at the same communication parameters.

Moreover, we numerically evaluate the 2-connectivity in a square area and a circular area. The simulation results show that the mobility and the "boundary effect" reduce the network's connectivity probability. Dynamic RWP motion model is most difficult to reach 2-connected network. In the UV network, the polygonal motion area model has a smaller limit to the UV node's motion range than the circular area model, and is closer to reality. Compared with the static uniform distribution

situation, the UV node positions have dynamic changes in the RWP motion mode, which provides more development space for UV networking in the future.

References

[1] Z. Yong *et al*., "Non-line-of-sight ultraviolet communication performance in atmospheric turbulence[J]," *China Commun.*, vol. 10, no. 11, pp. 52–57, 2013.

[2] A. Vavoulas, H. G. Sandalidis, and D. Varoutas, "Node isolation probability for serial ultraviolet UV-C multi-hop networks," *IEEE/OSA J. Opt. Commun. Netw.*, vol. 3, no. 9, pp. 750–755, 2011.

[3] G. Chen *et al*., "Path loss modeling and performance trade-off study for short-range non-line-of-sight UV communications[J]," *Opt. Express*, vol. 17, no. 5, pp. 3929–3940, 2009.

[4] T.-F. Zhao, Y. Wang, and Y.-Y. Gao, "Connectivity performance analysis of UV-NLOS communication metwork[A]," *J. Optoelectronics Laser*, vol. 26, no. 1, pp. 0609–0617, 2015.

[5] T. Zhao, Y. Xie, and Y. Zhang, "Connectivity properties for UAVs networks in wireless ultraviolet communication[J]," *Photonic Netw. Commun.*, 2018.

[6] D. M Reilly, D. T Moriarty, and J. A. Maynard, "Unique properties of solar-blind ultraviolet communication systems for unattended ground sensor networks[A]," *Proc.of SPIE[C]*, vol. 5611, pp. 244–254, 2004.

[7] Z. Xu, "Approximate performance analysis of wireless ultraviolet links[A]," in *Proc. IEEE Int. Conf.[C]*, 2007, pp. 577–580.

[8] C. Li, J. Li, Z. Xu, and J. Wang, "Study on the k-Connectivity of Ultraviolet Communication Network under uniform distribution of nodes in a circular region," in *Proc. IEEE 5th Int. Conf. Comput. Commun.*, 2019.

[9] G. Chen *et al*., "Path loss modeling and performance trade-off study for short-range non-line-of-sight ultraviolet communications[J]," *Opt. Express*, vol. 17, no. 5, pp. 3929–3940, 2009.

[10] A. Vavoulas, H. G. Sandalidis, and D. Varoutas, "Connectivity Issues for Ultraviolet UV-C Networks," *J. Opt. Commun. Netw.*, 2011.

[11] Q. He, B. M. Sadler, and Z. Xu, "Modulation and coding tradeoffs for non-line-of-sight ultraviolet communications[A]," *Proc. of SPIE[C]*, vol. 7464, pp. 74640H1–74640H12, 2009.

[12] E. Hyytia, P. Lassila, and J. Virtamo, "Spatial node distribution of the random waypoint mobility model with applications[J]," *IEEE Trans. Mobile Comput.*, vol. 5, no. 6, pp. 680–694, 2006.

[13] M. D. Penrose, "On k-connectivity for a geometric random graph[J]," *Random Struct. Algorithms*, vol. 15, no. 2, pp. 145–164, 2015.

[14] C. Bettstetter, G. Resta, and P Santi, "The node distribution of the random waypoint mobility model for wireless ad hoc networks[J]," *IEEE Trans. Mobile Comput.*, vol. 2, no. 1, pp. 25–39, 2003.

[15] E. Hyytia, P. Lassila, and J. Virtamo, "Spatial node distribution of the random waypoint mobility model with applications," *IEEE Trans. Mobile Comput.*, vol. 5, no. 6, pp. 680–694, 2006.

[16] C. Bettstetter and O. Krause, "On border effects in modeling and simulation of wireless ad hoc networks[A]," in *Proc. MWCN' 01 [C]*, Recife: IEEE Press, 2001.

[17] T. Zhao, Y. Xie, and Y. Zhang, "An area coverage algorithm for non-line-of-sight ultraviolet communication network," *Photonic Netw. Commun.*, vol. 32, no. 2, pp. 269–280, 2016.

[18] T. Zhao, Y. Gao, P. Wu, Y. Xie, and P. Song, "A networking strategy for three-dimensional wireless ultraviolet communication network," *Optik*, vol. 151, pp. 123–135, 2017.

[19] P. Shaik, K. K. Garg, and V. Bhatia, "On impact of imperfect channel state information on dual-hop non-line-of-sight ultraviolet communication over turbulent channel," *Opt. Eng.*, vol. 59, no. 1, pp. 016106-1–01610614, 2020.